

16. Yvon, K. in *Current Topics in Material Science* Vol. 3 (ed. Kaldis, E.) 53–129 (North-Holland, Amsterdam, 1979).
17. Chevrel, R., Sergent, M. & Prigent, J. Sur le nouvelles phases sulfurées ternaires du Molybdène. *J. Solid State Chem.* 3, 515–519 (1971).
18. Ritter, C., Gocke, E., Fischer, C. & Schollhorn, R. Neutron diffraction study of the crystal structure of lithium intercalated Chevrel phases. *Mater. Res. Bull.* 27, 1217–1225 (1992).
19. Linden, D. in *Handbook of Batteries* 2nd edn Ch. 23 (ed. Linden, D.) 23.3–23.22 (McGraw Hill, New York, 1994).

Acknowledgements

This work was partially supported by Advance Technology Upgrading (ATU) Ltd, Israel.

Correspondence and requests for materials should be addressed to D.A. (e-mail: aurbach@mail.biu.ac.il).

Importance of stirring in the development of an iron-fertilized phytoplankton bloom

Edward R. Abraham*, Cliff S. Law†, Philip W. Boyd‡, Samantha J. Lavender†§, Maria T. Maldonado||§ & Andrew R. Bowie#†

* National Institute for Water and Atmospheric Research (NIWA), PO Box 14-901, Kilbirnie, Wellington, New Zealand

† Plymouth Marine Laboratory, Prospect Place, The Hoe, Plymouth, Devon PL1 3DH, UK

‡ NIWA Centre for Chemical and Physical Oceanography, Department of Chemistry, University of Otago, Dunedin, New Zealand

|| Department of Biology, McGill University, 1205 Dr. Penfield Avenue, Montreal, PQ H2T 2V8, Canada

Department of Environmental Sciences, Plymouth Environmental Research Centre, University of Plymouth, Drake Circus, Plymouth PL4 8AA, UK

The growth of populations is known to be influenced by dispersal, which has often been described as purely diffusive^{1,2}. In the open ocean, however, the tendrils and filaments of phytoplankton populations provide evidence for dispersal by stirring^{3,4}. Despite the apparent importance of horizontal stirring for plankton ecology, this process remains poorly characterized. Here we investigate the development of a discrete phytoplankton bloom, which was initiated by the iron fertilization of a patch of water (7 km in diameter) in the Southern Ocean⁵. Satellite images show a striking, 150-km-long bloom near the experimental site, six weeks after the initial fertilization. We argue that the ribbon-like bloom was produced from the fertilized patch through stirring, growth and diffusion, and we derive an estimate of the stirring rate. In this case, stirring acts as an important control on bloom development, mixing phytoplankton and iron out of the patch, but also entraining silicate. This may have prevented the onset of silicate limitation, and so allowed the bloom to continue for as long as there was sufficient iron. Stirring in the ocean is likely to be variable, so blooms that are initially similar may develop very differently.

Remotely sensed ocean colour images show that there was an intense bloom in the vicinity of the SOIREE (Southern Ocean iron release experiment) site during March 1999 (Fig. 1). The phytoplankton bloom seen on 23 March has a peak chlorophyll *a* (chl_a) concentration of 3 mg m⁻³ (see Methods), which is extraordinary for this region^{6,7}, particularly as March is towards the end of the

growth season. To confirm that the feature was unusual, we analysed all the daily composite SeaWiFS data collected during the 1997–2000 September to March period, over the area between 134–146° E and 57–62° S. The mean concentration was 0.20 ± 0.06 mg chl_a m⁻³, and, apart from the images shown in Fig. 1 and occasional isolated pixels, there were no chlorophyll *a* concentrations greater than 1 mg m⁻³. Here we argue that the remotely sensed bloom is derived from the fertilization experiment. We show that stirring and diffusion of the SOIREE patch could have produced a filament of the dimensions seen in the images, and that there was sufficient iron in the fertilized patch to support the bloom during March.

The stretching of a tracer filament allows the strength of the stirring in a two-dimensional flow to be estimated (see Methods). A transect was made on 18 February, which showed that the patch which was responding to the fertilization was 30 km long (as evidenced by enhanced photosynthetic competency, $F_v/F_m > 0.3$). The only remotely sensed image of the entire bloom is from 23 March (Fig. 1d); by this time the patch appears as a 150-km-long ribbon of high chlorophyll *a* concentration. The change in the length of the patch over the intervening month (33 d) implies an effective strain rate of $\gamma = \ln(150/30)/33 = 0.05 \text{ d}^{-1} = 6 \times 10^{-7} \text{ s}^{-1}$. This is a minimum value, as the phytoplankton at the margins of the patch may be iron-limited, which would lead to the true length of the patch on 23 March being underestimated. By fitting gaussian profiles to the chlorophyll *a* concentration along cross-filament sections, the width of the bloom in the 23 March image is found to be $2\sigma_y = 4 \pm 2 \text{ km}$. This gives a diffusivity, $K_y = \sigma_y^2 \gamma$, of between 0.5 and 5 m² s⁻¹. These values of γ and K_y may be compared with estimates obtained from changes in the size and shape of the patch over the fortnight that it was followed by ship (Fig. 2). The patch's length increased over the course of the experiment, whereas its width stabilized at 4 km, the same as the width of the filament in the satellite images. The best fit to the length and width data is given by $\gamma = (8 \pm 3) \times 10^{-7} \text{ s}^{-1}$ and $K_y = 4 \pm 2 \text{ m}^2 \text{ s}^{-1}$, which agree very well with the values above. Here we use $\gamma = 8 \times 10^{-7} \text{ s}^{-1} = 0.07 \text{ day}^{-1}$ as the best estimate of the rate of stretching of the bloom.

The measured effective strain rate is close to the r.m.s. strain of $5.8 \times 10^{-7} \text{ s}^{-1}$ derived from a generic model of mesoscale turbulence⁸, and is of similar magnitude to the effective strain rate of $(3 \pm 0.5) \times 10^{-7} \text{ s}^{-1}$ determined by a tracer release within the ocean interior⁹. The horizontal diffusivity is lower than values found in previous open-ocean surface SF₆ releases: namely, $22 \pm 10 \text{ m}^2 \text{ s}^{-1}$ within an eddy in the North Atlantic Ocean¹⁰ and $25 \pm 5 \text{ m}^2 \text{ s}^{-1}$ in the equatorial Pacific Ocean (recalculated from ref. 11). Our value of the horizontal diffusivity is, however, within the range ($2\text{--}16 \text{ m}^2 \text{ s}^{-1}$) found at the length-scale $3\sqrt{2}\sigma_y = 8 \text{ km}$ from dye-release experiments in shelf seas¹². The plausibility of our derived values supports the assertion that the remotely sensed bloom was produced by the fertilization experiment.

The presence of horizontal stirring has implications for the growth of phytoplankton in an isolated patch. Stretching by the horizontal currents maintains cross-patch gradients against diffusion, causing continuing mixing along the sides of the filament. This results in a persistent dilution of the concentration at the patch centre¹³. If the net phytoplankton growth rate, μ , is higher than the strain rate, then the peak phytoplankton concentration within the patch will increase at the asymptotic rate $\mu - \gamma$ (see Methods). The carbon-based phytoplankton growth rate reached 0.19 d⁻¹ by the time the ship left the SOIREE site⁵ and the strain rate was $\gamma = 0.07 \text{ d}^{-1}$, so towards the end of the site occupation approximately 35% of the daily production was lost from the patch centre through horizontal dispersal. The losses due to dispersal were much higher than those from meso-zooplankton grazing (less than 0.01 d⁻¹, J. R. Zeldis, personal communication) and vertical sinking (less than 0.02 d⁻¹ (ref. 14)). Stirring rates are expected to be variable¹⁵, and are likely to be higher in regions with more eddy

§ Present addresses: Institute of Marine Studies, University of Plymouth, Drake Circus, Plymouth, Devon PL4 8AA, UK (S.J.L.); School of Marine Sciences, 5741 Libby Hall, University of Maine, Orono, Maine 04469, USA (M.M.)

activity than the SOIREE site, which was chosen for its weak surface currents⁵. If the strain rate is higher than the growth rate, then, from equation (2) in Methods, the phytoplankton concentration in an isolated bloom will never grow beyond $\gamma C_0/(\gamma - \mu)$, where C_0 is the background concentration. The importance of stirring poses a potential difficulty for iron fertilization. If a fertilized patch happened to be stirred rapidly then there would be little increase in phytoplankton stocks, despite the phytoplankton no longer being iron-limited. Because particle export from the surface layer has a strongly nonlinear dependence on algal concentration¹⁶, this may result in the added iron failing to induce a significant phytoplankton-mediated removal of carbon from the surface waters.

The iron fertilization caused the accumulation of between 600 and 3,000 t of algal carbon by the time of the 23 March image (see

Methods). On-deck incubations measured an intracellular phytoplankton uptake ratio of 3×10^{-6} mol Fe per mol C (the mean from days 5 and 12 of SOIREE was $(2.7 \pm 1.4) \times 10^{-6}$ mol Fe per mol C, for the $>2 \mu\text{m}$ phytoplankton size fraction, see Methods). If this uptake ratio remained constant, then the phytoplankton in the 23 March bloom would have contained between 8 and 40 kg of iron, an order of magnitude less than the 300 kg of dissolved iron which remained in the patch after the last infusion. There was a dissolved iron concentration of 1.1 nM at the centre of the fertilized patch at the end of the site occupation, and a background concentration of 0.1 nM. By this time there was an excess of organic iron-binding ligands⁵, maintaining the iron in solution. Towards the end of the site occupation there were minimal losses of dissolved iron from the surface layer, with the decrease in concentration being similar to what would be expected from horizontal

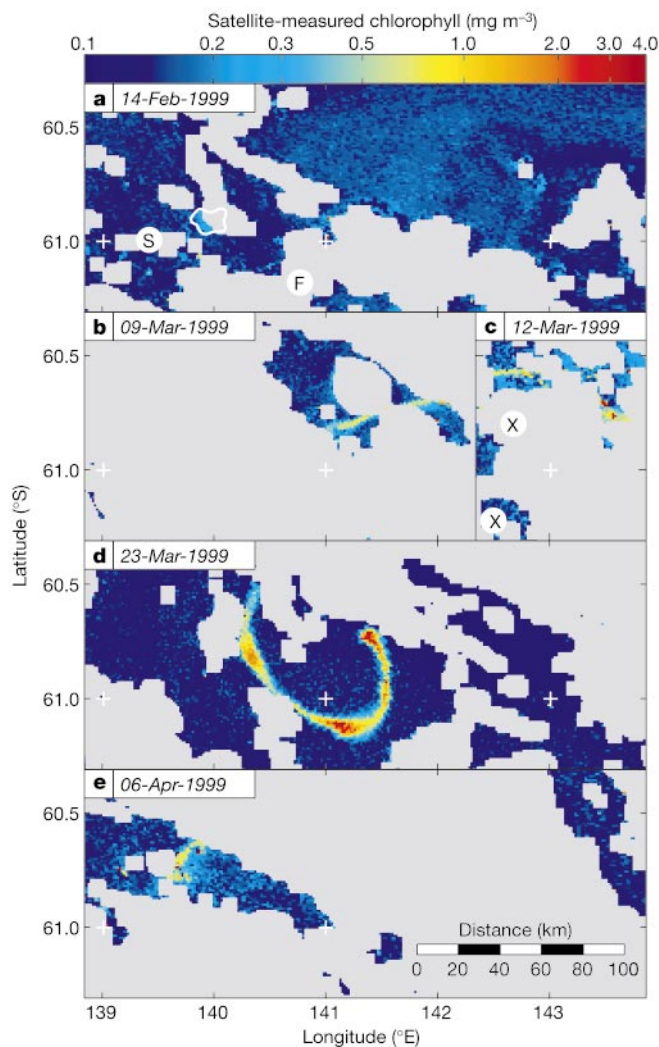


Figure 1 Images of the SOIREE bloom from the SeaWiFS ocean colour satellite. The region is usually cloudy, so during the months February–April only eight images of the bloom were obtained. Five of these are displayed here. The images show sea-surface chlorophyll *a* concentration on a logarithmic scale (see Methods), and areas that were obscured by cloud are marked in grey. Composite images of the bloom may be viewed at <http://seawifs.gsfc.nasa.gov>; the bloom is clearly visible in the March monthly climatology (1998–2000). **a**, The only image taken during the site occupation. S indicates the start of the SOIREE experiment, on 9 February 1999, and F indicates the position of the patch centre at the time of the final survey on 22 February. The white line is the edge of the patch, based on a shipboard survey at the time the image was taken. The chlorophyll *a* concentration within the contour is 0.1 mg m^{-3} higher than the background level.

Phytoplankton concentrations within the patch reached $2 \text{ mg chl a m}^{-3}$ by the time of the final survey. **b, c**, By 1 month after the initial release, the patch has become drawn out into a long streak. Another partial image was obtained on 7 March, which shows that the bloom extends no further to the west than seen here. X symbols mark the positions of temperature profiles taken on 3 March, which showed that the mixed layer was then 65 m deep. **d**, After 42 d, the fertilized patch has become stretched and folded into a 150-km-long ribbon. The area of the bloom is $1,100 \text{ km}^2$ ($>0.2 \text{ mg chl a m}^{-3}$), with the high-chlorophyll portion having an area of 230 km^2 ($>1.0 \text{ mg chl a m}^{-3}$). Two other partial images from 21 and 22 March show that this is close to being a complete image of the bloom. **e**, The bloom is still present 55 d after the initial release. This is the last image of the bloom that was obtained.

dispersal alone. The concentration of dissolved iron remaining in the patch centre at the time of the satellite images may then be calculated under the assumption that, apart from uptake required to maintain net phytoplankton growth, the dissolved iron was conserved. To keep the phytoplankton concentration steady at $2 \text{ mg chl} a \text{ m}^{-3}$, a growth rate of 0.10 d^{-1} (0.07 d^{-1} for dispersal and 0.03 d^{-1} to cover other losses such as sinking, which may not result in the iron being recycled), or $0.2 \text{ mg chl} a \text{ m}^{-3} \text{ d}^{-1}$, would have been required. Given an intermediate carbon-to-chlorophyll *a* ratio of $60 \text{ g C per g chl} a$, and the iron-to-carbon uptake ratio quoted above, only 3 pM d^{-1} of iron would have been needed by the phytoplankton at the bloom centre. It follows that there would still have been a peak concentration of 0.2 nM of dissolved iron within the filament on 23 March (see Methods), double the background concentration and sufficient to prevent severe iron limitation¹⁷. Although this calculation relies on the assumption that dissolved iron was retained within the surface layer, as was observed towards the end of the site occupation, a far higher loss rate of 11 pM d^{-1} would have been needed to reduce the concentration to background levels before 23 March. This suggests that, despite the stirring, there was enough dissolved iron in the fertilized patch to maintain increased phytoplankton growth during March.

The predominant taxa in the bloom when the ship left the SOIREE site were diatoms, which have a high silicate requirement, and the silicate concentration in the mixed layer decreased from 10 to $6 \text{ } \mu\text{M}$ during the 12-day site occupation. Although succession by other taxa is perhaps possible, phytoplankton blooms in open Southern Ocean waters are typically dominated by diatoms¹⁸, and so the development of the bloom for a further month suggests that stirring of the patch entrained enough silicate to support continued diatom growth. An algal uptake ratio of $0.18 \text{ mol Si per mol C}$ was measured during SOIREE, so a silicate uptake of $0.18 \text{ } \mu\text{M d}^{-1}$ would have been needed to maintain a growth rate of $0.2 \text{ mg chl} a \text{ m}^{-3} \text{ d}^{-1}$. The silicate drawdown can be estimated as the uptake rate divided by the strain rate; so a drawdown of $0.18/0.07 = 2.6 \text{ } \mu\text{M}$ is all that was required to supply sufficient silicate to the bloom. While the filament was being stirred there would not have been any silicate limitation, which helps to explain its longevity. An input of iron that was spread over an area with dimensions larger than the $\sim 100\text{-km}$ eddy length scale may result in a relatively short-lived bloom, as above this scale stirring is inefficient. Depending on their initial

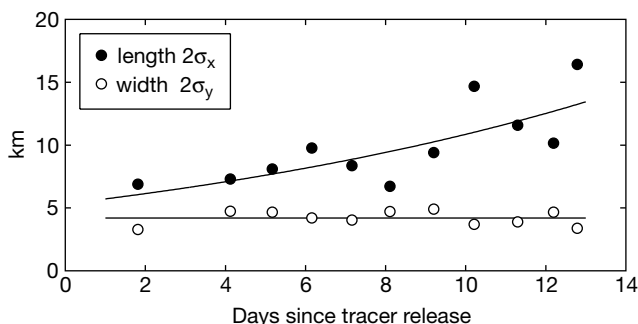


Figure 2 Changes in the size and shape of the fertilized patch following the initial infusion. A tracer, SF_6 , was added to the patch during the initial iron release⁵, enabling the patch to be mapped using an underway system³⁰. The width and length of the patch were determined by fitting a gaussian ellipsoid (equation (1) in Methods) to the SF_6 data from each daily survey, using a least-squares fitting procedure. The r.m.s. difference between the data and the best-fit ellipsoid was less than 15% of the peak SF_6 concentration for all the points shown. A best fit to the length and width of the patch after day 4 ($2\sigma_x \propto \exp(\gamma t)$, $2\sigma_y = 2(K_s/\gamma)^{1/2}$; shown by the lines) was used to estimate the strain rate and the diffusivity. The size of the patch that had above-background SF_6 concentrations was larger than the size obtained using the method described here. The patch defined by SF_6 concentrations above 8 fM reached a length of 30 km by 18 February (9 d after the initial release).

concentration, other nutrients such as silicate may then become limiting, leading to the decline of the bloom¹⁹.

We have presented the first (to our knowledge) experimental demonstration of the mesoscale stirring of a tracer patch in the surface ocean, a result made possible by the visibility of phytoplankton in satellite images. The stretching of the patch into a long filament agrees with recent theoretical analysis¹³, and supports the idea that the tendrils and whorls seen in naturally occurring plankton populations may be generated through horizontal stirring within the surface layer^{3,20,21}. The calculations presented here could be refined through the use of a numerical model that included a detailed representation of phytoplankton and iron dynamics. It is clear, however, that algal losses due to dispersal may dominate those from other processes, and that horizontal stirring will affect the concentration of nutrients within an isolated patch or filament. For these reasons, a consideration of stirring is essential to understanding the development of phytoplankton blooms in the open ocean. □

Methods

Satellite imagery

The SeaWiFS High-Resolution Picture Transmission (1-km resolution) data was obtained from the NASA GDAAC and processed using SeaAPS²². The images presented are level 2 chlorophyll *a* concentrations, estimated using the Ocean Chlorophyll 2 version 2 (OC2-v2) algorithm $\text{chl} a \text{ (mg m}^{-3}\text{)} = 10^{(0.2974 - 2.2429x + 0.8358x^2 - 0.0077x^3) - 0.0929}$, where x is the $490/555 \text{ nm}$ band ratio²³. The algorithm has not been extensively calibrated against *in situ* extracted-chlorophyll data from the Southern Ocean, although recent results suggest that it underestimates chlorophyll *a* concentrations there²⁴.

Dispersal of a tracer in the surface ocean

At scales greater than 1 km , and away from strong fronts, the currents in the surface ocean are approximately two-dimensional and divergence-free. The flow can then be locally resolved into a pure strain and a rotation. In a pure strain flow with a velocity $\mathbf{v} = (\gamma x, -\gamma y)$, where γ is the strain rate, a patch of tracer is stretched along the x -axis and squeezed in the y -direction. After an initial period of adjustment, an isolated patch of conserved tracer, $C(x,y,t)$, which is centred at the origin, becomes a gaussian ellipsoid;

$$C = (N/2\pi\sigma_x\sigma_y)\exp(-\frac{1}{2}(\frac{x^2}{\sigma_x^2} + \frac{y^2}{\sigma_y^2})) \quad (1)$$

where N is the total amount of tracer within the patch and $\sigma_x(t)$, $\sigma_y(t)$ are the standard deviations of the distribution in the x and y directions, respectively. The length of the patch increases exponentially at the rate γ , $\sigma_x(t) \propto \exp(\gamma t)$. In contrast, the width stabilizes at a steady value where the thinning effect of the strain balances the widening tendency of diffusion, $\sigma_y = (K_s/\gamma)^{1/2}$ (refs 9, 25). Once the width has stabilized, the peak concentration decreases at the rate γ . In ocean flows the strain is not constant, but an effective strain rate (more formally, a Lyapunov exponent) may be defined from the exponential growth in the length of a patch of tracer^{15,26}. Once the length of the filament becomes larger than the sizes of the eddies, the patch tends to be folded back upon itself and the tracer distribution loses its streakiness²⁶.

A pure-strain flow stretches a phytoplankton patch into a filament of the same dimensions as a patch of conserved tracer¹³. The change in the peak phytoplankton concentration in a fertilized bloom may be approximated by $dC/dt = \mu C - \gamma(C - C_0)$, where μ is the net growth rate the phytoplankton within the fertilized patch would have in the absence of dispersal; C_0 is the background concentration, which is assumed to be constant, and the second term represents losses due to dispersal. This equation has the solution

$$C(t) = \frac{\mu}{\mu - \gamma} C_0 \exp((\mu - \gamma)t) - \frac{\gamma}{\mu - \gamma} C_0 (\mu \neq \gamma), \quad C(t) = C_0 + \mu C_0 t (\mu = \gamma) \quad (2)$$

Algal carbon within the bloom

By integrating over the portion of the 23 March image (Fig. 1d) with concentrations greater than $0.2 \text{ mg chl} a \text{ m}^{-3}$, the near-surface chlorophyll *a* content of the bloom, per unit depth, is found to be 820 kg m^{-1} . There was an expendable bathythermograph (XBT) survey through the region of the bloom in early March (Fig. 1c), which showed that the surface waters were well mixed to a depth of 65 m , consistent with that found during the site occupation. It is unlikely that the mixed layer shoaled during March²⁷, and so the remotely sensed bloom can be assumed to have a 65-m extent. Given that the carbon-to-chlorophyll ratios remained in the range measured during SOIREE ($45\text{--}90 \text{ g C per g chl} a$), the 23 March bloom is estimated to have contained between $2,400$ and $4,800 \text{ t}$ of algal carbon. Areal algal carbon outside the fertilized patch was 1.6 g m^{-2} during the site occupation. If this remained steady, then there would have been $1,800 \text{ t}$ of algal carbon in the bloom waters in the absence of iron fertilization, implying that the fertilization caused the accumulation of between 600 and $3,000 \text{ t}$ of algal carbon by 23 March. Because the calibration of the SeaWiFS data is uncertain, the carbon-to-chlorophyll ratios are

estimated, and the true vertical structure of the bloom is unknown, these figures must be treated with caution, and they may be subject to revision.

Iron concentration within the patch

The rate of change of the dissolved iron concentration at the patch centre may be estimated as $dFe_{\text{max}}/dt = -\gamma(Fe_{\text{max}} - Fe_{\text{out}}) - P$, where Fe_{max} is the peak concentration within the patch; Fe_{out} is the background concentration; and P is a constant loss term, assumed to be the net rate of phytoplankton iron uptake. This equation has the solution $Fe_{\text{max}}(t) = (Fe_{\text{initial}} - Fe_{\text{out}} + P/\gamma) \exp(-\gamma t) + Fe_{\text{out}} - P/\gamma$, where Fe_{initial} is the peak iron concentration at $t = 0$.

The phytoplankton iron-uptake rate was obtained from the estimated net rate of carbon fixation and the Fe:C uptake ratio, which was measured by parallel incubation of ^{55}Fe ($0.2 \text{ nM } ^{55}\text{Fe}:10 \text{ }\mu\text{M EDTA}$) and $\text{H}^{14}\text{CO}_3^-$, as described previously²⁸. The Fe and EDTA addition resulted in a concentration of inorganic Fe (Fe') of 7.7 pM which mimicked the mean *in situ* Fe' concentration ($4.5 \pm 2.4 \text{ pM}$; P. L. Croot, personal communication). Underway dissolved iron was measured using a flow injection–chemiluminescence method²⁹.

With the values (see text) $Fe_{\text{initial}} = 1.1 \text{ nM}$, $Fe_{\text{out}} = 0.1 \text{ nM}$, $P = 0.003 \text{ nM d}^{-1}$, and $\gamma = 0.07 \text{ d}^{-1}$ it follows that after 28 d, $Fe_{\text{max}} = 0.20 \text{ nM}$. If the loss rate is $P = 0.011 \text{ nM d}^{-1}$ then after 28 d, $Fe_{\text{max}} = 0.10 \text{ nM}$.

Received 20 December 1999; accepted 4 September 2000.

- Kierstead, H. & Slobodkin, L. B. The size of water masses containing plankton blooms. *J. Mar. Res.* **12**, 141–147 (1953).
- Okubo, A. *Biomathematics Vol. 10, Diffusion and Ecological Problems* (Springer, Berlin, 1980).
- Gower, J. F. R., Denman, K. L. & Holyer, R. J. Phytoplankton patchiness indicates the fluctuation spectrum of mesoscale oceanic structure. *Nature* **288**, 157–159 (1980).
- Holligan, P. et al. A biogeochemical study of the coccolithophore, *Emiliania Huxleyi*, in the North Atlantic. *Glob. Biogeochem. Cycles* **7**, 879–900 (1993).
- Boyd, P. W. et al. A mesoscale phytoplankton bloom in the polar Southern Ocean stimulated by iron fertilization. *Nature* **407**, 695–701 (2000).
- Comiso, J. C., McClain, C. R., Sullivan, C. W., Ryan, J. P. & Leonard, C. L. Coastal Zone Color Scanner pigment concentrations in the southern ocean and relationships to geophysical surface features. *J. Geophys. Res.* **C 2**, 2419–2451 (1993).
- Sullivan, C. W. et al. Distributions of phytoplankton blooms in the southern ocean. *Science* **262**, 1832–1837 (1993).
- Haidvogel, D. B. & Keffer, T. Tracer dispersal by mid-ocean mesoscale eddies. Part I. Ensemble statistics. *Dyn. Atmos. Oceans* **8**, 1–40 (1984).
- Ledwell, J. R., Watson, A. J. & Law, C. S. Mixing of a tracer in the pycnocline. *J. Geophys. Res.* **C 103**, 21499–21529 (1998).
- Martin, A. P., Richards, K. J., Law, C. S. & Liddicoat, M. I. Horizontal dispersion within an anticyclonic mesoscale eddy. *Deep-Sea Res.* (in the press).
- Stanton, T. P., Law, C. S. & Watson, A. J. Physical evolution of the IronEx-I open ocean tracer patch. *Deep-sea Res.* **II 45**, 947–975 (1998).
- Okubo, A. Oceanic diffusion diagrams. *Deep-Sea Res.* **18**, 789–802 (1971).
- Martin, A. P. On filament width in oceanic plankton populations. *J. Plank. Res.* **22**, 597–602 (2000).
- Charette, M. A. & Buessler, K. O. Does iron fertilization lead to rapid carbon export in the Southern Ocean? *Geochem. Geophys. Geosyst.* [online] **1**, Paper number 2000GC000069 (<http://www.g-cubed.org>) (2000).
- Sundermeyer, M. A. & Price, J. F. Lateral mixing and the North Atlantic Tracer Release Experiment: observations and simulations of lagrangian particles and a passive tracer. *J. Geophys. Res.* **103**, 21481–21497 (1998).
- Jackson, G. A. A model of the formation of marine algal flocs by physical coagulation processes. *Deep-Sea Res.* **37**, 1197–1211 (1990).
- Olson, R. J., Sosik, H. M., Chekalyuk, A. M. & Shalapyonok, A. Effects of iron enrichment on phytoplankton in the Southern Ocean during late summer: Active fluorescence and flow cytometric analyses. *Deep-Sea Res.* (in the press).
- de Baar, H. J. W. & Boyd, P. W. in *The Dynamic Ocean Carbon Cycle: A Midterm Synthesis of the Joint Global Ocean Flux Study* (eds Hanson, R. B., Ducklow, H. W. & Field, J. G.) 61–140 (International Geosphere Biosphere Programme Book Series, Cambridge Univ. Press, Cambridge, 1999).
- Abbott, M. R., Richman, J. G., Letelier, R. M. & Bartlett, J. S. The spring bloom in the Antarctic Polar Frontal Zone as observed from a mesoscale array of bio-optical sensors. *Deep-Sea Res.* (in the press).
- Washburn, L., Emery, B. M., Jones, B. H. & Ondercin, D. G. Eddy stirring and phytoplankton patchiness in the subarctic North Atlantic in late summer. *Deep-Sea Res.* **I 45**, 1411–1439 (1998).
- Abraham, E. R. The generation of plankton patchiness by turbulent stirring. *Nature* **391**, 577–580 (1998).
- Lavender, S. J. & Groom, S. B. The SeaWiFS Automatic Data Processing System (SeaAPS). *Int. J. Remote Sensing* **20**, 1051–1056 (1999).
- O'Reilly, J. E. et al. Ocean color chlorophyll algorithms for SeaWiFS. *J. Geophys. Res.* **C 103**, 24937–24953 (1998).
- Moore, J. K. et al. SeaWiFS satellite ocean color data from the Southern Ocean. *Geophys. Res. Lett.* **26**, 1465–1468 (1999).
- Okubo, A. A note on horizontal diffusion from an instantaneous source in a nonuniform flow. *J. Oceanogr. Soc. J.* **22**, 1–6 (1966).
- Garrett, C. On the initial streakiness of a dispersing tracer in two- and three-dimensional turbulence. *Dyn. Atmos. Oceans* **7**, 265–277 (1983).
- Rintoul, S. R., Donguy, J. R. & Roemmich, D. H. Seasonal evolution of upper ocean thermal structure between Tasmania and Antarctica. *Deep-Sea Res.* **I 44**, 1185–1202 (1997).
- Maldonado, M. T., Boyd, P. W., Harrison, P. J. & Price, N. M. Co-limitation of phytoplankton growth by light and Fe during winter in the NE subarctic Pacific Ocean. *Deep-Sea Res.* **II 46**, 2475–2485 (1999).

- Bowie, A. R., Achterberg, E. P., Mantoura, R. F. C. & Worsfold, P. J. Determination of sub-nanomolar levels of iron in seawater using flow injection with chemiluminescence detection. *Anal. Chim. Acta* **361**, 189–200 (1998).
- Law, C. S., Watson, A. J., Liddicoat, M. I. & Stanton, T. Sulphur hexafluoride as a tracer of biogeochemical and physical processes in an open-ocean iron fertilisation experiment. *Deep-Sea Res.* **II 45**, 977–994 (1998).

Acknowledgements

We thank all the SOIREE team, particularly the captain and crew of RV *Tangaroa* for their assistance throughout the experiment; S. Nodder, R. Murdoch, A. Watson and T. Trull for experiment planning and coordination; and G. Jameson, M. Liddicoat and R. Ling for their work on the tracer release and mapping. We also thank S. Groom for additional interpretation of the remote sensing data; P. Nightingale for ARGOS data transfer; S. Rintoul for providing the XBT data; and M. Morris, C. Stevens and A. Martin for comments on the original manuscript. The SeaWiFS data, provided by the NASA DAAC/GSF and copyright of Orbital Imaging Corps and the NASA SeaWiFS project, was processed at CCMS-PML. E.A. and P.B. acknowledge the financial assistance of the NZ Public Good Science Fund for Antarctic research; C.L. thanks the UK Natural Environment Research Council for support; M.M. was supported by the Natural Sciences and Engineering Research Council of Canada (NSERC) and the Center for Environmental Bioinorganic Chemistry, Princeton (CEBIC); A.B. was supported by the University of Plymouth and Plymouth Marine Laboratory.

Correspondence and requests for materials should be addressed to E.A. (e-mail: e.abraham@niwa.cri.nz).

Effect of iron supply on Southern Ocean CO₂ uptake and implications for glacial atmospheric CO₂

A. J. Watson*, D. C. E. Bakker*, A. J. Ridgwell*, P. W. Boyd† & C. S. Law‡

* School of Environmental Sciences, University of East Anglia, Norwich NR4 7TJ, UK

† NIWA Centre for Chemical and Physical Oceanography, Department of Chemistry, University of Otago, Dunedin, New Zealand

‡ Centre for Coastal and Marine Studies, Plymouth Marine Laboratory, Prospect Place, The Hoe, Plymouth PL1 3DH, UK

Photosynthesis by marine phytoplankton in the Southern Ocean, and the associated uptake of carbon, is thought to be currently limited by the availability of iron^{1,2}. One implication of this limitation is that a larger iron supply to the region in glacial times³ could have stimulated algal photosynthesis, leading to lower concentrations of atmospheric CO₂. Similarly, it has been proposed that artificial iron fertilization of the oceans might increase future carbon sequestration. Here we report data from a whole-ecosystem test of the iron-limitation hypothesis in the Southern Ocean⁴, which show that surface uptake of atmospheric CO₂ and uptake ratios of silica to carbon by phytoplankton were strongly influenced by nanomolar increases of iron concentration. We use these results to inform a model of global carbon and ocean nutrients, forced with atmospheric iron fluxes to the region derived from the Vostok³ ice-core dust record. During glacial periods, predicted magnitudes and timings of atmospheric CO₂ changes match ice-core records well. At glacial terminations, the model suggests that forcing of Southern Ocean biota by iron caused the initial ~40 p.p.m. of glacial–interglacial CO₂ change, but other mechanisms must have accounted for the remaining 40 p.p.m. increase. The experiment also confirms that modest sequestration of atmospheric CO₂ by artificial additions of iron to the Southern Ocean is in principle possible, although the period and geographical extent over which sequestration would be effective remain poorly known.